JOURNAL OF CATALYSIS 98, 434–443 (1986)

The Influence of Oxonium Ion and Carbenium Ion Stabilities on the Alcohol/H-ZSM-5 Interaction[1]

M. T. ARONSON,* R. J. GORTE,* AND W. E. FARNETH†

*Department of Chemical Engineering, University of Pennsylvania, Philadelphia, Pennsylvania 19104; and †E. I. duPont de Nemours and Company, Central Research and Development Department, Experimental Station 356/231, Wilmington, Delaware 19898

Received June 28, 1985; revised November 26, 1985

We have examined the adsorption of methanol, ethanol, 1-propanol, 1-butanol, 2-propanol, and 2-methyl-2-propanol on H-ZSM-5 using temperature-programmed desorption (TPD) and thermogravimetric analysis (TGA). For each of the alcohols except 1-butanol, there exists a clearly defined desorption state corresponding to one alcohol molecule per Al atom in the zeolite. For 2-methyl-2-propanol and 2-propanol, this molecule at the Al site completely reacts to olefin products and water; however, reaction occurs at 295 K for 2-methyl-2-propanol, while 2-propanol does not react until 360 K. Most of the methanol, ethanol, and 1-propanol adsorbed at the Al sites at this coverage desorbs unreacted. A substantial amount of the 1-butanol adsorbed near the Al sites reacts, but differs from the other alcohols in that it reacts through a dibutyl ether intermediate. These results can be understood in terms of the stabilities of the carbenium ion intermediates which can be formed during reaction. A potential energy scheme, based on gas-phase proton affinity, is developed. This scheme provides a formalism for explaining relative reactivities of alcohols on H-ZSM-5 in TPD. © 1986 Academic Press, Inc.

INTRODUCTION

The dehydration of alcohols is one of the simplest acid-catalyzed reactions. In strong homogeneous acids, the reaction occurs through carbenium ion intermediates which can be stabilized and studied spectroscopically (*1–3*). Similar chemistry occurs in zeolites, and there have been numerous suggestions that carbenium ions or carbenium-like intermediates are involved (*4, 5*). In addition, evidence has been presented that 2-propyl carbenium ions,[2] formed by the dehydration of 2-propanol, can be stabilized in a H-ZSM-5 zeolite (*6*). It was found that 2-propanol reacted with a stoichiometry of one alcohol molecule for each Al atom in the zeolite structure under vacuum conditions. In another paper, it was reported that methanol did not react in H-ZSM-5 under vacuum conditions even though preferential adsorption near the Al sites was observed (*7*).

The differences in reactivity for methanol and 2-propanol are consistent with differences in the stability of the carbenium ion intermediates that could be formed from these alcohols. To further investigate the alcohol/zeolite interaction in H-ZSM-5, we have studied the adsorption and TPD behavior of a series of simple alcohols. Using temperature-programmed desorption (TPD) and thermogravimetric analysis (TGA), we have examined the effect of carbon chain length on the alcohol/zeolite interaction by investigating the primary alcohols: methanol, ethanol, 1-propanol, and 1-butanol. To determine the effect of carbenium ion stability on the alcohol/zeolite interaction, we have examined the adsorption and TPD of 2-methyl-2-propanol, 2-propanol, and 1-propanol. We find that a car-

---

[1] Supported by NSF, MRL Program, under Grant DMR 82-16718.

[2] We do not distinguish between a 2-propyl group bound to the zeolite framework in a covalent bond or in a completely ionic bond. The intermediate formed by 2-propanol decomposition exhibits the reaction properties of a true carbenium ion; therefore, we will refer to the intermediate as a carbenium ion, even though the extent of charge transfer is unknown.

0021-9517/86 $3.00

benium ion model gives a good description of the behavior within this series of simple alcohols. Furthermore, we develop a formalism for making this model quantitative.

EXPERIMENTAL TECHNIQUES

TPD and TGA experiments were carried out simultaneously using a microbalance mounted within a high vacuum chamber. The base pressure of this system was 1×10^{-8} Torr. It was pumped with a CTI cryotorr 7 with a rated pumping speed of approximately 10^3 liters per second for N_2. The sample weight could be continously monitored using a Cahn RG microbalance and the desorbing species could be measured using a UTI-100 quadrupole mass spectrometer. The sample temperature was measured with a thermocouple placed near the sample and the heating rate during the desorption was maintained at 5 K/min by a feedback controller.

Each of the different alcohols was adsorbed by exposing the sample to 10 Torr of vapor until no further uptake could be measured by the microbalance. To determine which chemical species were desorbing from the zeolite, we examined the mass range from 10 to 120 amu at 10 K intervals during the temperature ramp to measure the cracking patterns of each of the desorbing species. After the desorbing species were determined, the TPD experiments were repeated monitoring the major mass peak of each of the desorbing products. For all of the TPD curves shown in this paper, we have used the $M/E = 31$ peak for the alcohols and the $M/E = 41$ peak for the olefin products, except for ethene ($M/E = 28$), since these were always the largest peaks in the cracking pattern, in agreement with tabulated data. Comparison of TPD curves for several masses was used to identify the specific species desorbing in each peak. As many as five mass peaks could be monitored simultaneously using a multiplexer. Following an adsorption/desorption cycle, the weight of the zeolite returned to its original value. Over the course of an experimental sequence involving one cycle for each alcohol, the total mass change in the zeolite was less than 0.05%.

The zeolite samples were obtained as an NH_4-ZSM-5 powder from the Mobil Oil Company. Electron microscopy indicated that the zeolite particles were uniformly between 0.4 and 0.5 μm in diameter. X-Ray diffraction of these samples agreed with the published data for ZSM-5 (*8*). We checked the silica–alumina ratio by measuring the desorption of NH_3 from NH_4-ZSM-5 and obtained a ratio of 72, in good degreement with the value of 70 reported to us by Mobil. All experiments reported in this paper were performed on H-ZSM-5 prepared by heating NH_4-ZSM-5 to 700 K under vacuum.

RESULTS

Gravimetric Uptakes

The quantities of each alcohol that could adsorb onto H-ZSM-5 are shown in Table 1 along with the fraction of the zeolite pore volume that would be filled if each alcohol packed at its liquid density into the zeolite. A substantial fraction of the zeolite pore volume is filled for each of the alcohols after equilibrium is established with 10 Torr of vapor at 295 K; however, there are modest differences which can be explained

TABLE 1

Gravimetric Uptakes Obtained after Exposing the Sample to 10 Torr of Adsorbent Vapor at Room Temperature until no Further Weight Gain Could be Measured

Adsorbent	g adsorbed per 100 g zeolite at saturation	Molecules per Al atom at saturation[a]	Fraction pore volume filled at saturation[b]
Water	7.82	9.1	0.41
Methanol	10.24	6.7	0.68
Ethanol	12.83	5.9	0.86
1-Propanol	13.72	4.8	0.92
2-Propanol	13.10	4.6	0.88
1-Butanol	14.54	4.3	0.96
2-Methyl-2-propanol	11.26	3.3	0.75

[a] Determined using a silica–alumina ratio of 72.

[b] Assumes that each alcohol packed at its liquid density into the zeolite. A value of 0.19 cm^3/g was used for the porosity of H-ZSM-5.

in terms of the hydrophobicity of the ZSM-5 channels and the steric bulk of the alcohols. For the primary alcohols and water, a steadily increasing fraction of the pore volume is filled, going from 41% for water to 96% for 1-butanol. This is due to the increasingly organic nature of the larger alchols, which are stabilized in the pores by favorable interactions between the hydrocarbon chains and the channel walls. 2-Methyl-2-propanol and 2-propanol are less effective in filling the pores due to inefficient packing of bulky carbon skeletons in the small zeolite pores. Differences in the packing effectiveness are also observed in alkanes and we note that the ratio of pore volume filling for 2-methyl-2-propanol to 1-butanol is very similar to the ratio of filling for 3-methyl-pentane to *n*-hexane reported by Olsen *et al.* (*9*).

For each of the alcohols, between one and two alcohol molecules remained in the zeolite per Al atom after evacuation for 1.5 h at 295 K as shown in Table 2. The only exception was 1-butanol, for which 20 h of evacuation were needed to bring the coverage to 2.0 alcohol molecules per Al atom. Water could be completely removed by evacuation at room temperature; however, none of the alcohols could be removed beyond the one alcohol molecule per Al atom coverage, even after several days of evacuation at 295 K. Desorption to a coverage of two alcohol molecules per Al atom occurred rapidly for all alcohols. In the case of methanol, ethanol, 2-propanol, and 2-methyl-2-propanol, one of these two alcohol molecules could be removed by more prolonged evacuation. Previous work with infrared spectroscopy has shown that the adsorbed methanol (*7*) and 2-propanol (*6*) molecules are, in fact, interacting with the hydrogen cations which are associated with the Al atoms.

TABLE 2

TGA Results following Evacuation at Room Temperature

Adsorbent	g adsorbed per 100 g zeolite after 1.5 h evac.	Molecules per Al atom after 1.5 h evac.[a]
Water	0.0	0.0
Methanol	1.53	1.0
Ethanol	3.04	1.4
1-Propanol	5.70	2.0
2-Propanol	4.56	1.6
1-Butanol[b]	7.09	2.0
2-Methyl-2-propanol	3.52	1.0

[a] Determined using a silica–alumina ratio of 72.

[b] Evacuated 20 h.

TPD

The TPD results for each of the alcohols are shown in Figs. 1–6. The coverages are also shown in each figure as a function of temperature. For discussion, we have chosen to group the alcohols into two categories. The first category includes only primary alcohols and will be used to demonstrate the effect of chain length on the alcohol/zeolite interaction. The second category includes 1-propanol, 2-propanol, and 2-methyl-2-propanol and will be used to discuss the influence of carbenium ion stability on the alcohol/zeolite interaction.

Primary Alcohols

The primary alcohols that we studied include methanol, ethanol, 1-propanol, and 1-butanol. The TPD curves for methanol, ethanol, and 1-propanol are similar and indicate that these alcohols are relatively unreactive in H-ZSM-5. The curve for 1-butanol is complex and indicative of the trend to higher reactivity for the longer chain alcohols.

The TPD results for methanol, shown in Fig. 1, indicate that most of the methanol ($M/E = 31$) desorbs unreacted. We observed a single desorption state for methanol at 400 K, with only a very small amount of dimethyl ether ($M/E = 45$) forming at 620 K. Previous work by Ison and Gorte (*7*) using infrared spectroscopy showed that methanol is adsorbed at the Al sites within the zeolite. They reported that there were

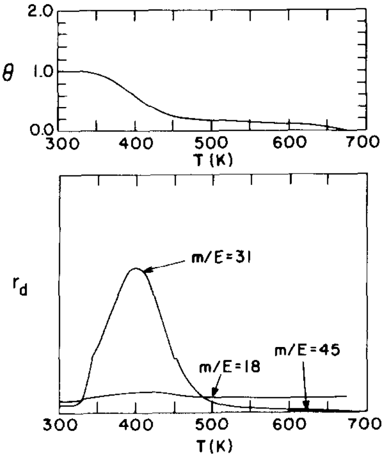

FIG. 1. TPD and TGA results for methanol on H-ZSM-5. Gravimetric uptakes are expressed as molecules per Al atom (θ) *M/E* ratios: methanol (31), water (18), and dimethyl ether (45).

two desorption states for methanol; however, they were not able to reduce the coverage of methanol on the sample to below two alcohol molecules per Al atom by evacuation at room temperature. They attributed the low-temperature desorption state to weakly adsorbed methanol, which we were able to remove at room temperature with the more efficient pumping in these experiments.

Ethanol desorption, shown in Fig. 2, also indicated that most of this alcohol desorbed before it could react. Unlike methanol, ethanol could not be evacuated to a coverage of one alcohol molecule per Al atom within reasonable (24 h) pumping times; however, the TPD curve did show that this additional ethanol (*M/E* = 31) was removed intact in a low-temperature desorption state at 370 K. The more strongly adsorbed ethanol existed at a stoichiometry of one alcohol molecule per Al atom and desorbed in a state centered at 440 K. A small fraction, approximately 10%, of this strongly adsorbed ethanol reacted to ethene (*M/E* = 28) and water (*M/E* = 18) during desorption.

The results for 1-propanol, shown in Fig. 3, are very similar to ethanol. After 90 min of evacuation, the zeolite sample still contained two molecules of 1-propanol per Al atom and one of them desorbed in a low-temperature state centered at 380 K. The more strongly bound 1-propanol (*M/E* = 31) is associated with a coverage of one alcohol molecule per Al atom and can be seen as a shoulder at 430 K on the more weakly bound state. Approximately 40% of the strongly adsorbed alcohol reacted during desorption to propene (*M/E* = 41) and water.

The TPD curves for 1-butanol are considerably more complex and are shown in Fig. 4. As with ethanol and 1-propanol, we were

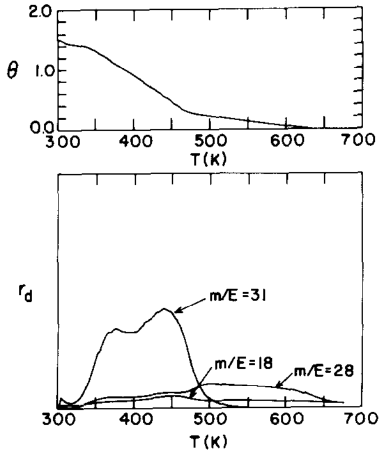

FIG. 2. TPD and TGA results for ethanol on H-ZSM-5. *M/E* ratios: ethanol (31) and ethene (28).

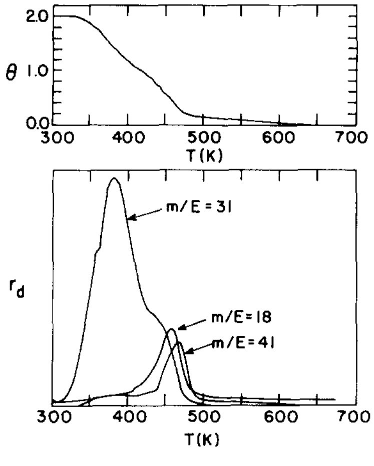

FIG. 3. TPD and TGA results for 1-propanol on H-ZSM-5. *M/E* ratios: 1-propanol (31) and propene (41).

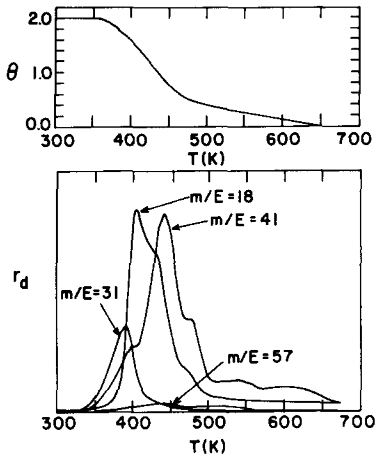

FIG. 4. TPD and TGA results for 1-butanol on H-ZSM-5. Small amounts of 1-butanol ($M/E = 31$) and dibutyl ether ($M/E = 57$) desorb from the sample unreacted. The majority of the 1-butanol reacts to form olefin products ($M/E = 41$) and water. The cracking patterns indicated that the peak at 440 K is due to butene, while the peaks at 480 and 540 K are due to higher molecular weight olefins.

unable to evacuate the sample to a coverage of one alcohol molecule per Al atom. Unlike ethanol and 1-propanol, a substantial fraction of even the second alcohol molecule per Al atom was able to react. Starting with a coverage of two 1-butanol molecules per Al atom, we observed the desorption of some unreacted 1-butanol ($M/E = 31$) at 390 K. However, the rapid rise in the water desorption at this temperature showed that reaction was occurring simultaneously. At 430 K, we observed a second desorption peak for water as a shoulder on the main water desorption curve. As the temperature increased further, dibutyl ether ($M/E = 57$) and butene ($M/E = 41$) were observed at 440 K along with higher molecular weight olefins ($M/E = 41$) at 480 and 540 K. The assignment of the desorption peak at 440 K to butene and the desorption peaks at 480 and 540 K to higher molecular weight olefins was made by examining the cracking patterns of the desorbing species. It should be noted that the feature at 400 K on the $M/E = 41$ desorption curve is due to the cracking pattern for 1-butanol and does not correspond to another product peak.

The following picture of 1-butanol adsorption emerges from these results. At room temperature after 20 h of evacuation, two alcohol molecules are present at each Al site. At a relatively low temperature, the rate of bimolecular reaction to dibutyl ether becomes competitive with the rate of desorption of 1-butanol. This is indicated by the sharp water peak at 400 K. This sharp water peak accounts for very close to one half of the water desorbing from the sample. Only a small amount of the bulky dibutyl ether can desorb from the sample before undergoing further dehydration to butene. A substantial fraction of the butene then undergoes further reaction to form higher molecular weight olefins.

Primary, Secondary, Tertiary Alcohols

In order to examine the influence of carbenium ion stability on the alcohol/zeolite interaction, we have compared the adsorption of 1-propanol, 2-propanol, and 2-methyl-2-propanol. As we discussed in the last section, 1-propanol is relatively unreactive. Although more than one 1-propanol molecule per Al atom was present in the zeolite at room temperature, the more strongly adsorbed alcohol molecules, which existed at a coverage of one per Al atom, desorbed in a separate state. Only about 40% of the strongly adsorbed alcohol desorbed as propene and water.

The results were very different for 2-propanol and 2-methyl-2-propanol, as shown in Figs. 5 and 6. The initial coverage, after 90 min evacuation for 2-methyl-2-propanol and after 20 h for 2-propanol, was one molecule per Al atom. No unreacted alcohol was observed during desorption for either of these alcohols. For 2-propanol, only water and propene desorbed from the sample at 400 and 405 K, respectively. For experiments run after shorter evacuation times in which the initial coverage of 2-propanol was greater than one alcohol molecule per Al atom, some unreacted 2-propanol desorbed at 360 K, as previously reported by Grady and Gorte (*6*). For 2-methyl-2-propanol the water desorption feature is small. Reaction apparently occurs even at room temperature and most of the water formed during the dehydration reaction desorbs during the evacuation prior to the TPD experiment. With longer evacuation times, the small water peak at 360 K can be eliminated completely. Furthermore, we saw only a small amount of butene desorbing from the sample at 350 K. The majority of desorbing olefin, as determined by the cracking patterns of the desorbing species, was octenes at 430 K presumably formed by the dimerization of butenes.

DISCUSSION

All of the molecules we have examined, with the exception of 1-butanol, show a discrete desorption event from a state with a stoichiometry of one alcohol molecule per Al atom. For 2-propanol and 2-methyl-2-propanol, the strongly adsorbed species reacts completely and desorbs as olefin and water. For methanol, ethanol, and 1-propanol, the strongly adsorbed species reacts only to a small extent, and most of the alcohol desorbs intact. For ethanol and 1-propanol, adsorption exceeds the 1 : 1 stoichiometry after 1.5 h evacuation at room temperature. Even in these cases, however, alcohol desorption from the state with 1 : 1 stoichiometry gives a TPD peak that is clearly separated from the alcohol adsorbed in excess of this stoichiometry. For ethanol, for example, the break in the desorption curve at approximately 380 K corresponds in temperature with the 1 : 1 stoichiometry in the TGA output (Fig. 2).

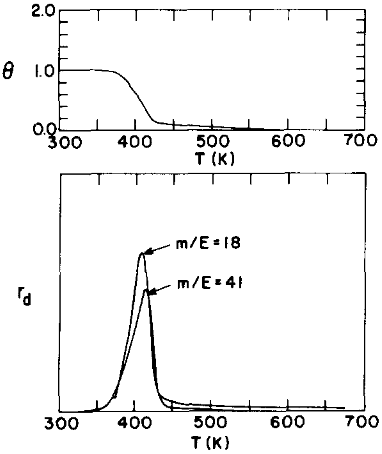

FIG. 5. TPD and TGA results for 2-propanol on H-ZSM-5. *M*/*E* ratio: propene (41).

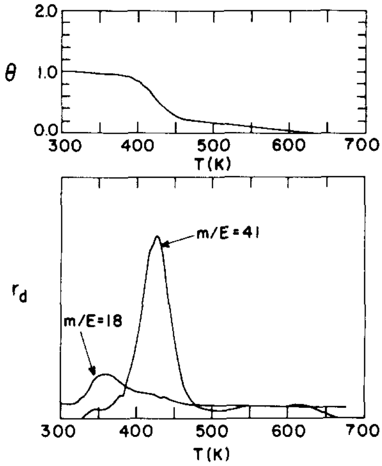

FIG. 6. TPD and TGA results for 2-methyl-2-propanol on H-ZSM-5. Most of the water formed during the dehydration reaction desorbs prior to the TPD experiment. All desorbing olefins were monitored using *M*/*E* = 41; however, the cracking patterns indicated that the peak at 350 K is due to butene, while the peaks at 430 K and 600 K are due to higher molecular weight olefins.

The demonstration of a 1 : 1 stoichiometry between tightly bound alcohol molecules and framework Al atoms over a range of alcohol structures is an important observation. It suggests that one can construct a general model for alcohol chemisorption on H-ZSM-5 that focuses on the interaction of the hydroxyl functionality with the acid sites at each Al atom in the zeolite framework. Other work from our group has shown that the acidic protons at these sites *are* involved in alcohol chemisorption. For example, infrared results for propene adsorption on D-ZSM-5 showed that all the deuterium cations were incorporated into the adsorbed species (*6*). Prior evidence from other groups has indicated that the Brønsted acid sites in H-ZSM-5 are isolated and uniformly active.[3] These points suggest the following scheme for rationalizing our results:

$$\mathrm{HROH} + \mathrm{ZOH} \underset{k_{(-1)}}{\rightleftharpoons} \mathrm{HROH}_2^+ + \mathrm{ZO}^-$$

$$\mathrm{HROH}_2^+ + \mathrm{ZO}^- \overset{k_{(2)}}{\rightleftharpoons} \mathrm{HR}^+ + \mathrm{H_2O} + \mathrm{ZO}^-$$

$$\mathrm{HR}^+ + \mathrm{ZO}^- \rightleftharpoons \mathrm{R} + \mathrm{ZOH}$$

Scheme I

This scheme implies that the primary interaction between the zeolite (ZOH) and the alcohol (HROH) is proton transfer to form an oxonium ion/framework anion pair ($\mathrm{HROH}_2^+ + \mathrm{ZO}^-$). One such ion pair will be formed for each Brønsted acid site in the zeolite. As shown in Scheme I, this complex may decompose back to free alcohol or dehydrate via a carbenium ion intermediate when the system is heated. The competition between these two decomposition routes will be sensitive to structure, since the energy required for $k_{(2)}$ will fall with increased carbenium ion stability. The general features of this mechanism for alcohol dehydration in zeolites have been pointed out by Jacobs (*4*) and alluded to by others (*5*).

In order to put this model on a more quantitative basis, we would like to be able to evaluate the relative energies of each structure in Scheme I as R is varied. To begin, one could imagine the first step of Scheme I as a hypothetical gas-phase proton transfer creating two separated ions. In this context, the enthalpy change of step 1 can be thought of as the difference between the two proton affinities:

$$\begin{array}{rl}
\mathrm{ZOH}_{(g)} \rightarrow \mathrm{ZO}^- + \mathrm{H}^+ & \Delta H = -\mathrm{P.A.}_{(\mathrm{ZO}^-)} \\
\mathrm{HROH}_{(g)} + \mathrm{H}^+ \rightarrow \mathrm{HROH}_2^+ & \Delta H = \mathrm{P.A.}_{(\mathrm{HROH})} \\
\hline
\mathrm{ZOH}_{(g)} + \mathrm{HROH}_{(g)} \rightarrow \mathrm{HROH}_2^+ + \mathrm{ZO}^- & \Delta H = \mathrm{P.A.}_{(\mathrm{HROH})} - \mathrm{P.A.}_{(\mathrm{ZO}^-)}
\end{array}$$

In a similar way, the energy of forming a carbenium ion from an olefin can be estimated as the difference between the proton affinities of the olefin and the zeolite framework anion.

Of course, on an absolute thermochemical basis, this gas-phase picture of zeolite acid-base chemistry is not justified. Solvation energies and interaction energies inside the zeolite will be large. However, one may make the model more reasonable by building the interaction energies into a thermochemical cycle as shown below. In this cycle, the binding energy of HROH in H-ZSM-5 is considered to be the sum of two proton affinities (P.A.) and an interaction energy ($\Delta H_{\mathrm{interaction}}$). Starting with the noninteracting alcohol and zeolite in the upper left, a gas-phase proton transfer can be imagined leading to the hypothetical "free" ions in the lower right. One can then imagine allowing these species to come together to adopt whatever geometry is preferred by proton transfer within the zeolite. Absolute values for the vertical legs of this cycle are not known.[4] However, the sum of the two vertical legs can be calculated for a given alcohol if the binding energy and the proton affinity of that alcohol are both known. Once the sum ($\Delta H_{\mathrm{interaction}} + \mathrm{P.A.}_{(\mathrm{ZO}^-)}$) is

---

[3] Evidence that H-ZSM-5 can behave as a collection of isolated, uniform active sites comes from Ref. (*10*). However, it seems likely that whether this is true or not is a sensitive function of preparation and calcination conditions, e.g., Ref. (*11*).

[4] However, one nice feature of this formalism is that the vertical legs of the cycle may be susceptible to theoretical calculation. Derouane and Fripiat (*12*) have recently published ab initio calculations that yield values for $\mathrm{PA}_{\mathrm{ZO}^-}$ for various models of zeolite framework acid sites.

established for one adsorbate, the binding energy can be calculated for any other molecule whose proton affinity is known by assuming that $\Delta H_{\text{interaction}}$ is independent of R. Proton affinities for all of the alcohols and olefins we have investigated are known (*13*).

$$\begin{tikzcd}
HROH_{(g)} + ZOH \arrow[r, "\Delta H_{\text{binding}}"] \arrow[d, "-PA_{(ZO^-)}"'] & HROH_2^+ \ldots\ldots ZO^- \\
HROH_{(g)} + ZO^- + H^+ \arrow[r, "PA_{HROH}"'] & HROH_2^+ + ZO^- \arrow[u, "\Delta H_{\text{interaction}}"']
\end{tikzcd}$$

The molar heat of adsorption for methanol on H-ZSM-5 is approximately 15 kcal/mole (*14*). With this value and the procedure discussed above, one can estimate the sum of the vertical legs of the cycle to be 170 kcal/mole, since the proton affinity of methanol is 185 kcal/mole. To calculate a binding energy for ethanol, then, one would use the known proton affinity (190 kcal/mole) and the sum of the vertical legs (170 kcal/mole) to determine that ΔH for step 1 in Scheme I is -20 kcal/mole. To complete the determination of the thermochemistry of Scheme I with ethanol, we note that the standard heat of dehydration of ethanol to H_2O and C_2H_4 is 11 kcal/mole and the proton affinity of ethylene is 163.5 kcal/mole. These values allow $C_2H_4 + H_2O$ (+11 kcal/mole) and $CH_3CH_2^+ + ZO^-$ (+17.5 kcal/mole) to be placed on a potential energy scale relative to $ZOH + C_2H_5OH$. Similar calculations have been carried out with all the alcohols to generate Fig. 7.

Figure 7 is useful for understanding a wide variety of data on absorbate/H-ZSM-5 interactions. It predicts that the binding energies of all the oxonium ions should be similar and in a range consistent with the intact desorption events observed in TPD. It predicts that the only large difference in heats of chemisorption among the hydroxy compounds we have examined will be between water and methanol. This is consistent with the observation that only water can be completely removed from the zeolite at room temperature. The differences in chemistry among the alcohols are especially well accounted for. The model clearly shows that the competition between dehydration and intact desorption will be controlled in large measure by carbenium ion stability. For methanol, the carbenium ion is significantly less stable than the free alcohol. Hence, heating of the oxonium ion/framework anion pair leads to reverse proton transfer and desorption of intact alcohol ($k_{(-1)}$). For ethanol and 1-propanol, the carbenium ion channel ($k_{(2)}$) begins to become competitive; and for 2-propanol, where Fig. 7 predicts that the carbenium ion is actually more stable than the free alcohol, dehydration is observed exclusively. For 2-methyl-2-propanol, the carbenium ion is only 8 kcal/mole less stable than the oxonium ion, consistent with dehydration at room tem-

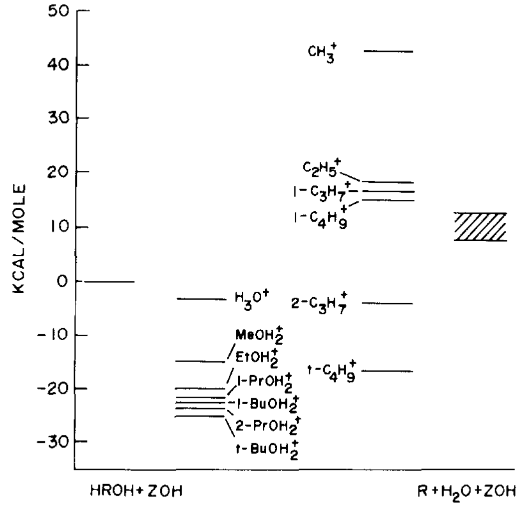

FIG. 7. Potential energy diagram of alcohol/H-ZSM-5 interactions. The adsorption of alcohols and olefins on the zeolite is assumed to occur predominantly through proton transfer, allowing the use of known proton affinities to calculate relative heats of formation.

perature. For 1-butanol, the picture is more complicated and would require including biomolecular dehydration chemistry on the potential diagram. Reading the surfaces from the olefin side, one predicts that carbenium ion formation will be endothermic for ethene but exothermic for propene, in accord with the observation of much faster oligomerization chemistry by the latter at 295 K (*15, 16*).

This formalism can be used in a predictive sense as well. For example, benzene, toluene, and *p*-xylene have proton affinities of 186, 193, and 194 kcal/mole, respectively (*13*). Using methanol as the anchor as we have in Fig. 7, one predicts enthalpies of adsorption for these compounds of 16, 23, and 24 kcal/mole, in remarkable agreement with the measured values of 17, 19, and 21 kcal/mole (*17*). The binding energy of ammonia is predicted to be 35 kcal/mole, again in excellent agreement with the measured differential enthalpy of adsorption at low coverage of 34.5 kcal/mole (*18*).

Our results inidcate that there is an attraction for at least a second molecule at the acid site since evacuation of this second molecule is much slower than is observed for the additional molecules which adsorb in the presence of the vapor. Our model for H-ZSM-5 acidity also provides a formalism for a qualitative understanding of adsorption at these higher coverages. In the gas phase, neutral molecules tend to cluster around charged species, although the interaction energy falls off rapidly with increasing cluster size (*19*). For example, when H_2O clusters around K^+ ions, the binding energy falls off by roughly 2.5 kcal/mole per H_2O adsorbed (*20*). In the zeolite analogy, the second, third, etc. molecule bound per Al atom will be associated with a growing cluster about the primary proton transfer complex. Each additional alcohol molecule will be less tightly held.

Several major assumptions have gone into this model for H-ZSM-5 acidity and one should be cautious about overinterpreting Fig. 7. First, we have assumed that all enthalpy changes due to interaction between various adsorbates and the zeolite framework are structure independent. However, it has been common practice in solution-phase ion chemistry to ignore differences in solvation energies in constructing structure–reactivity relationships. Where data exists, it has often been shown that this assumption is justified at least for compounds with similar structures (*21*). Relative carbenium ion stabilities, for example, are essentially the same in the gas phase, water, and SO_2ClF (*22*). In the context of Fig. 7, this assumption is likely to be most misleading in predicting the enthalpy difference between oxonium ions and carbenium ions because the structural change here is most severe. It is likely that the relative oxonium ion stabilities and the relative carbenium ion stabilities are more accurate because they represent smaller structural changes.

Second, the value of 15 kcal/mole, which we used as our estimate of the heat of adsorption for methanol, should be considered a lower limit. It is an integral heat of adsorption calculated from heat of immersion data, and the differential heat of adsorption for binding of the first alcohol molecule per Al atom may be significantly larger. It is unlikely, however, that the binding energy of the first methanol molecule is greater than 25 kcal/mole since this is what one would predict for a "normal" desorption event from a nonporous surface giving $T_{\max} = 400$ K under the conditions of our experiments. The effects of diffusion and readsorption from porous samples tends to raise desorption temperatures, indicating that the binding energy is less than 25 kcal/mole (*23, 24*). Finally, the scheme ignores entropy effects.

While the formalism developed in this paper has proven successful in picturing adsorption of a variety of compounds on H-ZSM-5, it is useful to examine cases where the formalism breaks down. *n*-Hexane, for example, probably has a lower proton affinity than water, yet it binds to H-ZSM-5 with a substantial chemisorption energy (*25*). For the alkanes in general, the binding presumably is not proton-transfer induced, but results from favorable lateral interactions between the extended hydrocarbon chains and the channel walls and among the chemisorbed molecules. The failure of 1-butanol to conform to the general picture observed here is probably related to the increased importance of these terms for longer hydrocarbon chains.

SUMMARY

We believe that for a range of alcohols, and perhaps for a variety of other structural types of adsorbates as well, the principal interaction in chemisorption on H-ZSM-5 at 295 K is proton transfer. Proton-transfer chemisorption creates localized oxonium ion/framework anion pairs. The binding energies of these oxonium ions are related to gas phase proton affinities of the alcohols. Adsorption above the one alcohol molecule per Al level is weaker and can be removed during prolonged evacuation times at room temperature under vacuum. Adsorbed oxonium ions decompose either by reverse proton transfer or by dehydration via a carbenium ion when heated. The relative rates of these competing channels depend principally on the stability of the intermediate carbenium ion. We have proposed a general formalism for systematizing observations on H-ZSM-5 chemisorption behavior.

ACKNOWLEDGMENTS

We are grateful to the Mobil Oil Corporation for supplying us with the ZSM-5 samples. We also would like to acknowledge Mr. Willis Dolinger for his technical assistance and for his help in setting up the experiments.

REFERENCES

1. Morrison, R. T., and Boyd, R. N., "Organic Chemistry," 3rd ed., pp. 166–175, 200–201, 521–523. Allyn and Bacon, Boston, 1978.
2. Olah, G. A., *Agnew. Chem. Int. Ed. Engl.* **12,** 173 (1973).
3. Olah, G. A., Schilling, P., Staral, J. S., Halpern, Y., and Olah, J. A., *J. Amer. Chem. Soc.* **97,** 6807 (1975).
4. Jacobs, P. A., "Carboniogenic Activity of Zeolites," p. 100. Elsevier, Amsterdam, 1977.
5. Deane, S., Wilshier, K., Western, R., Mole, T., and Seddon, D., *J. Catal.* **88,** 499 (1984).
6. Grady, M. C., and Gorte, R. J., *J. Phys. Chem.* **89,** 1305 (1985).
7. Ison, A., and Gorte, R. J., *J. Catal.* **89,** 150 (1984).
8. Olson, D. H., Haag, W. O., and Lago, R. M., *J. Catal.* **61,** 390 (1980).
9. Olson, D. H., Kokotailo, G. T., Lawton, S. L., and Meier, W. M., *J. Phys. Chem.* **85,** 2238 (1981).
10. Olson, D. H., Haag, W. O., and Largo, R. M., *J. Catal.* **61,** 390 (1980); Guisnet, M., Cormerais, F.-X., Chen, Y.-S., Perot, G., and Freund, E., *Zeolites* **4,** 108 (1984).
11. Choudhary, V. R., and Nayak, V. S., *Zeolites* **5,** 15 (1985).
12. Derouane, E. G., and Fripiat, J. G., *Zeolites* **5,** 165 (1985).
13. Aue, D. H., and Bowers, M. T., "Gas Phase Ion Chemistry," Vol. 2, p. 1. Academic Press, New York, 1979.
14. Messow, U., Quitzsch, K., and Herden, H., *Zeolites* **4,** 255 (1984).
15. van den Berg, J. P., Wolthuizen, J. P., Claque, A. D. H., Hays, G. R., Huis, R., and van Hooff, J. H. C., *J. Catal.* **80,** 130 (1983).
16. Cant, N. W., and Hall, W. K., *J. Catal.* **25,** 161 (1972).
17. Pope, C. G., *J. Phys. Chem.* **88,** 6312 (1984).
18. Vederine, J. C., Auroux, A., and Coururier, G., (T. E. Whyte, Jr., Ed.), *ACS Symp. Ser.* **248,** 253 (1984).
19. Kebarle, P., *Annu. Rev. Phys. Chem.* **28,** 445 (1977).
20. Sunner, J., and Kebarle, P., *J. Amer. Chem. Soc.* **106,** 6315 (1984).
21. Arnett, E. M., and Pienta, N. J., *J. Amer. Chem. Soc.* **102,** 3329 (1980).
22. Saunders, M., Chandrasekhar, J., and Schleyer, P. von R., *in* "Rearrangements in Ground and Excited States" (P. de Mayo, Ed.), Vol. 1, p. 1. Academic Press, New York, 1980
23. Gorte, R. J., *J. Catal.* **75,** 164 (1982).
24. Demmin, R. A., and Gorte, R. J., *J. Catal.* **90,** 32 (1984).
25. Flanigen, E. M., Bennett, J. M., Grose, R. W., Cohen, J. P., Patton, R. L., Kirchner, R. M., and Smith, J. V., *Nature (London)* **271,** 512 (1978).